Article

Heptacoordinated W(IV) Cyanido Supramolecular Complex Trapped by Photolysis of a [W(CN)$_6$(bpy)]$^{2-}$/Zn^{2+} System

Maciej Hodorowicz,* Janusz Szklarzewicz, Mariusz Radoń, and Anna Jurowska

Read Online

ACCESS | Metrics & More | Article Recommendations | SI Supporting Information

ABSTRACT: The synthesis and single-crystal X-ray structure of the supramolecular complex {[Zn]$_{1.5}$[Zn(H$_2$O)][W(CN)$_5$(OH)$_2$][W(CN)$_5$(OH)(H$_2$O)]} (**1**) are reported. We found that photolysis of PPh$_4$[W(CN)$_6$(bpy)] in the presence of Zn(NO$_3$)$_2$ aq results in formation of a porous supramolecular network (channels with a volume of 44.1% of the unit cell volume) with all cyanido ligands involved in W−CN−Zn bridges. Complex **1** crystallizes in the $Pm\bar{3}n$ space group with a cell volume of 20560.7 Å^3 with three Zn and two W distinct coordination spheres. All water coordinated to Zn is directed into holes of 8.27 Å in diameter in porous **1**. The presence of Zn cations during the photolysis results in isolation and structural characterization of unique seven-coordinate complex ions, [W(CN)$_5$(OH)$_2$]$^{3-}$ and [W(CN)$_5$(OH)(H$_2$O)]$^{2-}$, which were earlier only postulated as the photolysis intermediates. Quantum chemical calculations for isolated [W(CN)$_5$(OH)$_2$]$^{3-}$ and [W(CN)$_5$(OH)(H$_2$O)]$^{2-}$ ions show that their ideal pentagonal bipyramid geometries around W(IV) atoms are stable only in the crystal phase due to interactions with Zn^{2+} cations. The energy difference between the most stable distorted pentagonal bipyramid and that found in the crystal structure is predicted to be only 4 or 11 kcal/mol for each ion, respectively. The tungsten and zinc sites present in the crystal lattice of **1** pose different acidic properties for their aqua ligands with theoretically estimated pK_a values of ca. 7 and 8, respectively.

From chaos to rare Pm-3n symmetry
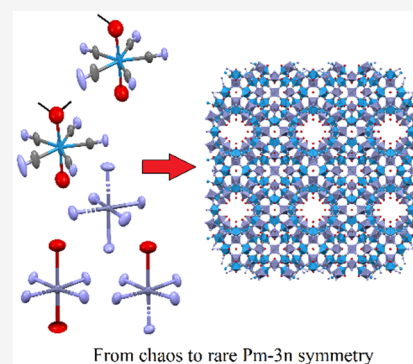
INTRODUCTION

The photochemistry of cyanido complexes of transition metals could be divided into substitutional (within d−d transition region) or redox (in charge-transfer, CT, region). In the case of the hexacyanido complex of tungsten, it was found that the primary photolysis of [W(CN)$_6$(bpy)]$^-$ (bpy denotes 2,2′-bipyridine) results in W(V) reduction to W(IV) with preserving the anion structure.[1−3] The prolonged photolysis or photolysis of [W(CN)$_6$(bpy)]$^{2-}$ results in bpy molecule release in the first step. After bpy release, it is believed that the sequence of processes occur, depending on pH. This sequence is identical to that found in substitutional photolysis of octacyanidotungstate or, generally speaking, octacyanidometallates [M(CN)$_8$]$^{4-}$ (M = Mo or W) and leads to formation of penta- and tetra-cyanides of general formula [M(CN)$_5$O]$^{3-}$ and [M(CN)$_4$O(L)]$^{n-}$ (where L = O^{2-}, OH$^-$ or H$_2$O depending on pH, n = 4, 3 or 2, respectively).[4−34] Only hexacoordinated complexes as penta- and tetra-cyanido complexes of Mo(IV) and W(IV) were isolated and characterized, including X-ray crystal structure determination.[35−41] The process of coordination number decrease from 8 to 6 is only postulated, and thus a theoretical approach was used to predict the formulas of formed intermediates.[42] Both heptacyanido complexes of formula [M(CN)$_7$L]$^{n-}$ (where L = OH$^-$, O^{2-}, n = 4, 5 respectively) and hexacyanido complexes of formula [M(CN)$_6$OL]$^{n-}$ (L = H$_2$O, OH$^-$ or O^{2-}, n = 3−5) were postulated on the basis of spectral changes during photolysis. There is, however, no direct information about the intermediates. In the case of [W-

(CN)$_6$(bpy)]$^{2-}$, the [W(CN)$_6$(OH)$_2$]$^{4-}$ intermediate was postulated prior to pentacyanido complex formation.[2] On the other hand, on the basis of theoretical calculations, the octacoordinated W(IV) was excluded, and heptacoordinated hexacyanides were postulated.[42] However, these calculations were based on the assumption that the reverse process, cyanation of [W(CN)$_5$O]$^{3-}$ (cyanation product of [W-(CN)$_4$OL]$^{n-}$ systems) to [W(CN)$_8$]$^{4-}$, is a stepwise process through hexa- and hepta-cyanido intermediates with also a stepwise increase of the coordination number from 6 to 8. The complex isolated by us is a very important indication of how the photolysis and/or synthesis of [W(CN)$_8$]$^{4-}$ from low cyanido precursors take place.

The cyanido complexes of transition metals are of crucial importance in the synthesis of supramolecular structures of molecular magnetic materials. In most cases, the symmetric cyanido complexes of the type [M(CN)$_8$]$^{n-}$ or [M(CN)$_6$]$^{n-}$ are used (M = Mo, W, Nb, Fe, Co, etc.). The [W(CN)$_6$(bpy)]$^-$ system was also utilized in this investigation due to the presence of bpy (bpy = 2,2′-bipyridine), which could decrease the

dimensionality of supramolecular nets formed.[43−46] As W(V) is of low interest in these investigations (because such an anion poses only −1 charge), we decided to investigate the structure of the W(IV) analogue as possessing more options in supramolecular net formation. As the Zn salt forms polymers with $[W(CN)_6(bpy)]^{2−}$ of very low solubility, we had to slow down the formation of crystals, and we used as the precursor the $[W(CN)_6(bpy)]^−$ ion salt, which has a much better solubility of its Zn salt, and we kept the system at room temperature. After 6 months of crystal growth, we have found that W(V) was photochemically reduced to W(IV) as expected, but the bpy ligand was also released. As a result, we trapped the intermediate product of tungsten(IV) photolysis, which brought new information on the photolysis products of not only $[W(CN)_6(bpy)]^{2−}$, but also $[M(CN)_8]^{4−}$ systems.

Recently, we have found that geometries of cyano complexes for Mo(IV) show deformations from those expected for symmetrical systems. Especially, we have proved this for the $[Mo(CN)_6]^{2−}$ ion, when the crystallographic data are contrary to quantum calculations.[47] As in **1** a very symmetrical pentagonal bipyramid is observed for both W centers, we decided to use quantum calculations to determine if this is geometrically preferred for isolated $[W(CN)_5(OH)_2]^{3−}$ and $[W(CN)_5(OH)(H_2O)]^{2−}$ ions, or is forced (or stabilized) by the formation of a net of cyanido-bridges to Zn^{2+} cations.

■ EXPERIMENTAL SECTION

$Zn(NO_3)_2 \cdot 6H_2O$, agar, and MeCN were of analytical grade (Aldrich or Alfa Aesar) and were used as supplied. Ethanol (98%) of pharmaceutical grade was from Polmos and was used as supplied. All other solvents were of analytical grade (Aldrich) and were used as supplied. $(PPh_4)_2[W(CN)_6(bpy)] \cdot 4H_2O$ was synthesized using a literature method.[1,3,48,49] $AsPh_4[W(CN)_6(bpy)]$ was synthesized as described earlier.[3]

Synthesis of PPh_4[W(CN)_6(bpy)]. Salt was synthesized by three different methods: (a) 0.1 g (0.11 mM) of $AsPh_4[W(CN)_6(bpy)]$ was dissolved in MeOH/H_2O (1:1, v/v) and was passed through an ion-exchange column (Amberlite IR 120 in H^+ form). Next to the solution of $H[W(CN)_6(bpy)]$ 0.1 g (0.3 mM) of Ph_4Cl was added, and the mixture was left in the dark for crystallization. Yield 83 mg, 90%. (b) The procedure was analogous to the described in ref 3, but $(PPh_4)_2[W(CN)_6(bpy)] \cdot 4H_2O$ was used instead of $(AsPh_4)_2[W(CN)_6(bpy)] \cdot 4H_2O$. Yield 16%. H_2O/MeCN (1:1 v/v) mixture (ca. 10 mL). (c) 0.5 g (0.4 mM) of $(PPh_4)_2[W(CN)_6(bpy)] \cdot 4H_2O$ was dissolved in a H_2O/MeCN (1:1 v/v) mixture (ca. 30 mL), acidified with 1 mL of 0.2 M HNO_3 and 1 mL of 30% H_2O_2 was added. The mixture was heated to ca. 90 °C up to formation of an almost colorless (light pink) solution. This was left to crystallization in the dark. The next day, well-shaped crystals were filtered off, washed with water, and dried. Yield 0.308 g, 92%.

Elemental analysis, IR and UV−vis spectra of all samples prepared as described in a−c were identical within experimental error.

Synthesis of {[Zn]_{1.5}[Zn(H_2O)][W(CN)_5(OH)_2][W(CN)_5(OH)(H_2O)]} (1). A hot (ca. 50 °C) saturated solution of 21 mg of $PPh_4[W(CN)_6(bpy)]$ in MeCN/H_2O (1:1 v/v) with agar was placed in a glass vial of ca. 6 mm diameter. After cooling and gel formation, the saturated solution of agar in hot (ca. 80 °C) water was layered on top of a previous layer to form ca. 1 cm layer and was almost immediately cooled in refrigerator (−20 °C) for 2 min. Then a hot (ca. 80 °C) solution of $Zn(NO_3)_2$ aq (1 g in 10 mL of water with ca. 0.1 g of agar) was layered on a previous agar layer to form a new layer of thickness of ca. 2 cm. Again, the vial was then kept for ca. 2 min in the refrigerator for freezing. The vial was then left for ca. 6 months for crystal growth at the laboratory table (at room temperature, ca. 22 °C) far from a window. The very dark red crystal was then separated manually and used in crystal structure measurement.

Crystallographic Data Collection and Structure Refinement. Diffraction intensity data for single crystal of the new compound **1** were collected at 130 K on the Oxford Diffraction Super Nova diffractometer using monochromatic Mo Kα radiation, λ = 0.71073 Å. Cell refinement and data reduction were performed using firmware.[50] Positions of all of non-hydrogen atoms were determined by direct methods using SHELXL-2016/6.[51,52] All non-hydrogen atoms were refined anisotropically using weighted full-matrix least-squares on F^2. Refinement and further calculations were carried out using SHELXL-2016/6.[51,52] Partial occupancy of the Zn3 atom was revealed after refinement of the displacement parameter (a.d.p.). Because of the high symmetry and the special position, its occupancy rate of 0.12 (1/8) was assigned to provide a reasonable isotropic a.d.p. Our attempts to localize the hydrogen atoms of the hydroxyl groups and solvent water molecules failed. The poor "visibility" of hydrogen atoms is mainly due to two main factors. The first one is a large disorder of water molecules despite measuring at −143.15 °C, which is manifested by the presence a residual (about $1e^−$) electron density at a distance of about 1 Å around oxygen atoms. This is due to the presence of large voids in the structure and the associated high rotation freedom of the molecules. The second factor is the high absorption (80.45 $cm^{−1}$) of X-rays caused by the presence of heavy atoms in the structure and the large size of the crystal. It was not decided to attribute the electron density around oxygen atoms as potential hydrogen atoms because it would not significantly improve the image of the structure, and in addition such a solution would force the binding on water molecules, which would significantly worsen structural parameters such as R_1 or wR_2. Additionally, there were disordered water solvent molecules present in the structure. Since no obvious major site occupations were found for those molecules, and it was not possible to model them and they were removed using the SQUEEZE procedure[53] implemented in the PLATON package.[54−57] The figures were made using Diamond ver. 4.6.3 software.[58] CCDC 2002709 contains the supplementary crystallographic data for **1**. These data can be obtained free of charge from The Cambridge Crystallographic Data Centre via www.ccdc.cam.ac.uk/data_request/cif.

Quantum-Chemical Calculations. Geometry optimizations of $[W(CN)_5(OH)_2]^{3−}$ and $[W(CN)_5(OH)(H_2O)]^{2−}$ ions, assuming either a singlet (S = 0) or triplet (S = 1) spin state, were carried out at the DFT:PBE0/def2-TZVP level of theory[59] with the TURBO-MOLE-7 package.[60] The conductor-like screening model (COSMO, with $\varepsilon = \infty$)[61] was used in order to roughly simulate the charge screening effect of the crystal surrounding.[62] Numeric integration was performed on the m5 grid, and the SCF convergence threshold was set to $10^{−8}$ in atomic units. The geometry convergence criteria were $10^{−6}$ and $10^{−4}$ (in atomic units) for the energy change and maximum norm of Cartesian gradient, respectively. The initial geometries of anions were based on the crystal structure here reported (with added H atoms of OH/OH_2 ligands). Analytic harmonic frequency calculations demonstrate that the optimized geometries are energy minima (in a few cases, imaginary frequencies related to rotations of OH group were apparent, but additional verification showed that this is an artifact related to the interplay of solvation model and numeric integration, as no energy lowering was observed when the structure was distorted along the indicated modes; the attempts to reoptimize such distorted structure led back again to identical geometry). All calculations for seven-coordinate complexes were spin-unrestricted, and both closed-shell ($\langle S^2 \rangle \approx 0$) and open-shell ($\langle S^2 \rangle > 0$) singlet solutions were identified. Theoretical pK_a values were estimated using the proton exchange method[63] with respect to the $[W(CN)_4O(H_2O)]^{2−}/[W(CN)_4O(OH)]^{3−}$ acid−base pair as the reference. Computed results may be accessed as an ioChem-BD collection under the following link: https://doi.org/10.19061/iochem-bd-7-3.

■ RESULTS AND DISCUSSION

General Remarks to the Synthesis. The conversion method described in the literature of W(IV) to W(V) is the oxidation of $(AsPh_4)_2[W(CN)_6(bpy)] \cdot 4H_2O$ in acidic medium using $MnO_4^−$ ions.[3] We have found that due to the formation of Mn^{2+} precipitation of $\{[fac-(H_2O)_3Mn^{II}-(\mu-NC)_3-$

$W^{IV}(CN)_3bpy]\cdot4.5H_2O\}_\infty$ 2D coordination polymer is observed, rapidly reducing the yield of the synthesis.[43] Moreover, the salt has to be recrystallized to remove impurities. However, the recrystallization results in partial reduction of the complex, additionally reducing the yield of the synthesis. This forced us to use another oxidant, H_2O_2, typically used in the synthesis of $[M(CN)_8]^{3-}$ ion salts possessing a similar redox potential as that of the $[W(CN)_6(bpy)]^{2-/-}$ system. The excess of H_2O_2 prevents reduction of formed W(V) during crystallization, and as a result high yield is achieved. As W(V) salts are light sensitive, all manipulations were done in the dark.[2,3,42]

Complex **1** could not be prepared from any known W(IV) cyanido complex. The reaction of the known tungsten(IV) pentacyanide ion with Zn^{2+} results in cyano ligand release and formation of tungstates. It is caused by fact that the $[W(CN)_5O]^{3-}$ ion is unstable in acidic media (caused by presence of $ZnCl_2$ or $Zn(NO_3)_2$ salts). Forcing of alkaline pH results in zinc hydroxides precipitation. We also could not use a second stable cyanido complex - octacyanidotungstates (IV or V) due to the insolubility of Zn salts. We decided to use a second known stable high cyanido complex of tungsten, the hexacyanido complexes. The addition of Zn^{2+} ion salts to solutions of $[W(CN)_6(bpy)]^{2-}$ results in the formation of very fine crystals of an almost insoluble product. On the other hand, addition to $[W(CN)_6(bpy)]^-$ results in the formation of a much better soluble zinc salt. Thus, to obtain **1** we were forced to use the W(V) complex. Still crystallization of W(V) salt is observed when both anions and zinc cations are present in solution and formation of **1** was obscured. We used agar gel to separate Zn^{2+} anions from $[W(CN)_6(bpy)]^-$ anions and to slow down formation of unwanted crystals of W(V) zinc salt. After 6 months of crystal growth, in conditions described in experimental part, we have found that W(V) was photochemically reduced to W(IV) as expected, but the bpy ligand was also released. Because of diffused natural light of low intensity, the process was slow. As a result we trapped the dark red intermediate product of tungsten(IV) photolysis **1**. This was separated manually from gel and transferred for further measurements. The yield of synthesis is small, annd in each experiment performed (we repeated the synthesis several times) only several big crystals were formed of micrograms quantity in total. Most of the formed crystals were very small, and we could not separate them manually. Because of similar solubility of agar–agar and complex, we could not also separate them by filtration. This did not allow us to perform elemental analysis or measure a diffuse reflectance spectrum.

Description of the Structure. Complex **1** crystallizes in the rare cubic space group $Pm\overline{3}n$. The asymmetric entity of the unit cell consists of the two W and three Zn atoms (W/Zn ratio of 2:3) and six cyanido ligands. In addition, the asymmetric part of the elementary cell contains six oxygen atoms as −OH groups or water molecules, some of which coordinate to metal atoms, while others are water of crystallization. The crystallographic data and detailed information on the structure solution and refinement for **1** are given in Table 1. The molecular structure of the crystals of **1** with the atom labeling scheme is illustrated in Figure 1. Selected bond parameters are summarized in Table S1 in the Supporting Information. In the structure of the title compound, there are two types of tungsten anions, with different coordinating environment, but both taking the geometry of a very symmetrical pentagonal bipyramid (Figure 2a,b, Figure 3a,b). In $[W(CN)_5(OH)_2]^{3-}$ ion (W2) the sum of angles C−W−C is 360.03°, which means an almost ideal flat pentagonal

Table 1. Crystal Data and Structure Refinement for 1

|	**1**
empirical formula	$C_{240}N_{240}O_{146}W_{48}Zn_{45.93}$
formula weight	20407.72
temperature (K)	130.2(2)
wavelength	0.7107 Å
crystal system	cubic
space group	$Pm\overline{3}n$
unit cell dimensions	$a = 27.3955(2)$ Å
	$b = 27.3955(2)$ Å
	$c = 27.3955(2)$ Å
	$\alpha = 90°$
	$\beta = 90°$
	$\gamma = 90°$
volume	20560.7(5) Å^3
Z	1
density (calculated)	1.648 Mg/m^3
absorption coefficient	8.045 mm^{-1}
$F(000)$	9218
crystal size	$0.300 \times 0.300 \times 0.200$ mm^3
theta range for data collection (°)	3.155−30.092
index ranges	$-38 \leq h \leq 38$
	$-30 \leq k \leq 31$
	$-35 \leq l \leq 38$
reflections collected	84576
independent reflections	5223 [$R(int) = 0.0646$]
completeness to theta = 25.242°	99.2%
absorption correction	semiempirical from equivalents
max and min transmission	1.00000 and 0.34894
refinement method	full-matrix least-squares on F^2
data/restraints/parameters	5223/0/154
goodness-of-fit on F^2	1.041
final R indices [$I > 2\sigma(I)$]	$R_1 = 0.0514$, $wR_2 = 0.1262$
R indices (all data)	$R_1 = 0.0717$, $wR_2 = 0.1395$
largest diff peak and hole	3.728 and −2.981 e/Å^3
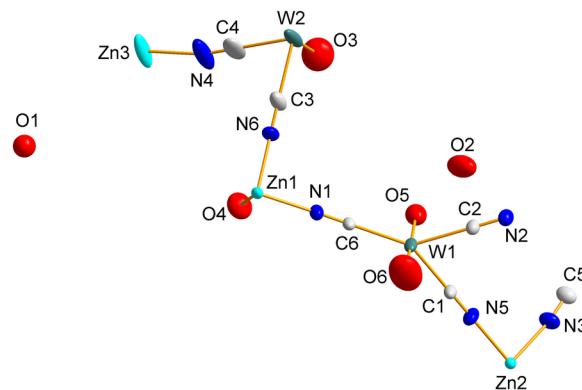
Figure 1. Asymmetric part of the unit cell $[0 \leq x \leq 1/2$ and $0 \leq y \leq 1/2$ and $0 \leq z \leq 1/4$ and $z \leq \min(x, 1/2 - x, y, 1/2 - y)]$ of the compound **1** with adopted atomic numbering scheme. All non-hydrogen atoms are represented at 30% probability thermal ellipsoids.

plane, with the difference between the largest and smallest angle C−W−C being only 1.2°. A similar situation is the case with the second anion, that is, $[W(CN)_5(OH)(H_2O)]^{2-}$ (W1). The sum of angles C−W−C is 359.52°, and the biggest and the smallest angle C−W−C also differ by 1.2°. The tungsten atom W1 is connected to three zinc atoms Zn1 and two zinc atoms Zn2 via cyanide bridges (Figure 2c), while in the indirect environment of W2, also via CN bridges, there are two atoms Zn1, two Zn2, and
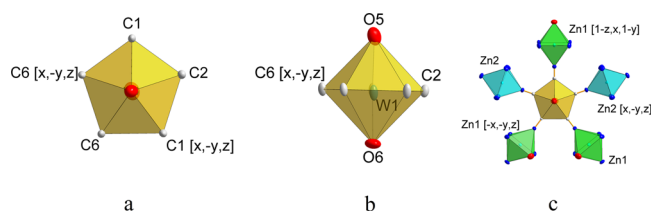
Figure 2. (a, b) The environment of coordination of W1 cations, (c) the cyanide bridges and the nearest metallic surroundings of cation W1 (node 1). All atoms are represented at 30% probability thermal ellipsoids.
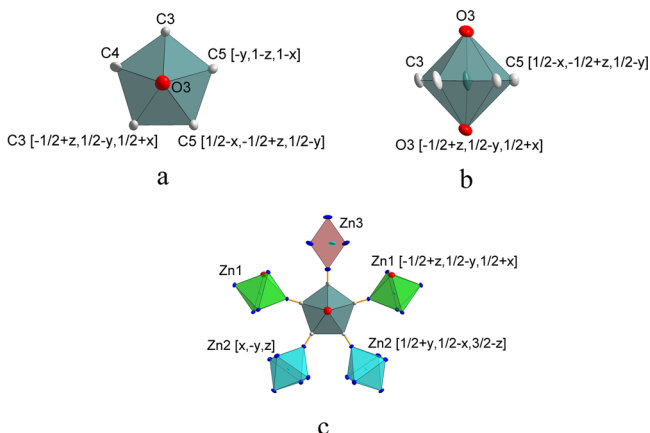

Figure 3. (a, b) The environment of coordination of W2 cations, (c) the cyanide bridges and the nearest metallic surroundings of cation W2 (node 2). All atoms are represented at 30% probability thermal ellipsoids.

one zinc atom Zn3 (Figure 3c). Since the hydroxyl oxygen atom O3 in the tungsten W2 environment is multiplied by symmetry, both bond lengths W−OH are equal and are 2.110 Å. In the case of the environment of tungsten W1, it can be seen that the bond length W−OH (O6) is 2.034 Å. This reduction of the bond length between the tungsten atom W1 and hydroxyl oxygen O6 is related to the influence of the presence in the *trans* position of the water molecule O5 being at a distance of 2.256 Å from W1 and causing a slight axial distortion of the pentagonal bipyramid (see Table S1). Although there is no direct analogy here, similar elongation and consequently shortening of the opposite *trans* bond can also be observed in teracyanido complexes of tungsten and molybdenum with patterns $[M(CN)_4O(OH)]^{3-}$ and $[M(CN)_4O(H_2O)]^{2-}$, in which M=O bond occurs.[64] Because of the lack of literature data for this type of structure with the tungsten atom, a direct comparison can only be made with corresponding molybdenum complexes, keeping in mind that complexes of both metals (W, Mo) usually have almost the same metal−ligand bond distances.[64] In complex ions type $[Mo(CN)_4O(OH)]^{3-}$, the length of bond Mo−OH differs depending on the cation and takes values in the range from 2.077 to 2.15 Å,[65−67] while in the case of bond Mo−H2O, the length of the bond changes in the range from 2.271 to 2.96 Å.[40,67,68] Comparing W−OH and W−H2O bond distances in W1 and W2 with that of tetracyanido complexes, it can be seen that due to the longer W−OH bond distance compared to that of W=O the decrease of W−OH (2.110 Å in W2) and W−H2O (2.256 Å in W1) in the *trans* position is observed. However, this difference is not very significant.

In this structure, three different types of coordination of atoms Zn can be distinguished. The zinc atom Zn2 is coordinated in ideal octahedral geometry by a total of six nitrogen atoms (three symmetrically dependent N3 and N5 atoms each) of cyanide ligands, and the angles in this polyhedron differ from 90° by not more than 1.4° (Figure 4a). The bond lengths Zn2−N are 2.117
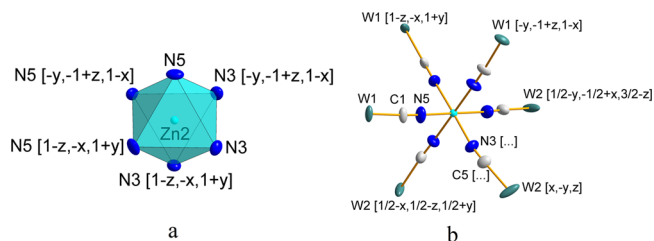

Figure 4. (a) The environment of coordination of Zn2 cations (b) the cyanide bridges and the nearest metallic surroundings of cation Zn2 (node 3). All atoms are represented at 30% probability thermal ellipsoids.

and 2.105 Å for N3 and N5, respectively. The geometry of the coordination environment around the Zn1 atom is also octahedral, but due to the presence of the H2O particle as a ligand, a slight deviation from the ideal geometry is observed (Figure 5a). In particular, the relatively long bond Zn−H2O of
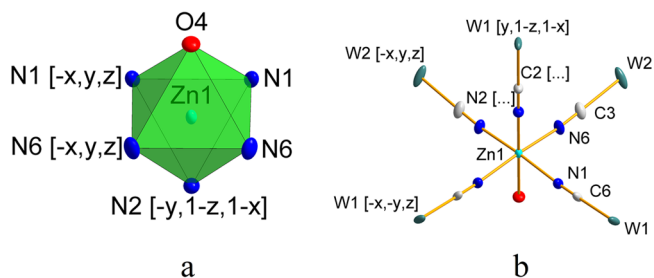

Figure 5. (a) The environment of coordination of Zn1 cations, (b) the cyanide bridges and the nearest metallic surroundings of cation Zn1 (node 4). All atoms are represented at 30% probability thermal ellipsoids.

2.245 Å is the reason for shortening the bond Zn1−N2 (2.089 Å). In the case of the remaining bonds Zn1−N (N6 and N1), their lengths are in the range between 2.111 and 2.123 Å.

At first glance, the third zinc atom Zn3 seems to have a coordinating environment with square geometry. Although in the case of the zinc atom, such a geometry is allowed, which is confirmed by literature data, unfortunately, most probably the Zn3 environment adopts the geometry of a strongly axially elongated octahedron. While the base of the mentioned one is very well marked and consists of symmetrically dependent nitrogen atoms N4 of cyanide ligands (Figure 6), axial positions are most likely occupied by heavily disordered water molecules. This disorder concerns the incomplete occupation of the axial positions of the coordination polyhedron, and in order to enable the publication of the structure, it was decided to remove this residual water (electron density) using the SQUEEZE procedure[53] of the PLATON software.[54−57] When analyzing the metallic surroundings of individual zinc atoms, it can be seen that Zn1 is connected by cyanide bridges with three W1 and two W2 atoms (Figure 4b), Zn2 has three W1 and W2 atoms each (Figure 5b), while Zn3 is indirectly connected with four symmetrically dependent W2 atoms (Figure 6). In the drawings,
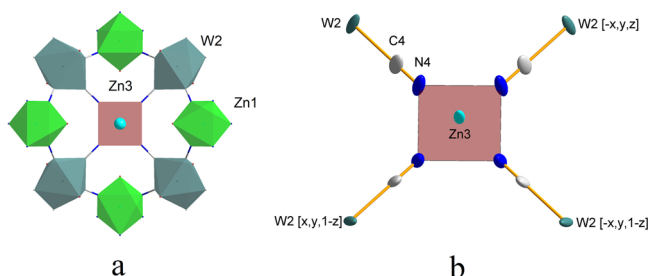
Figure 6. (a) The environment of coordination of Zn3 cations, (b) the cyanide bridges and the nearest metallic surroundings of cation Zn3 (node 5). All atoms are represented at 30% probability thermal ellipsoids.

the following colors are used to distinguish the coordination polyhedrons for each metallic center: yellow − W1, dark blue − W2, green − Zn1, light blue − Zn2, and red − Zn3.

The structure of the compound under investigation, although it does not belong to the MOF type, is highly porous. It has channels with a volume of 9059.7 Å^3, which is as much as 44.1% of the unit cell volume (Figure 7). The calculation is based on
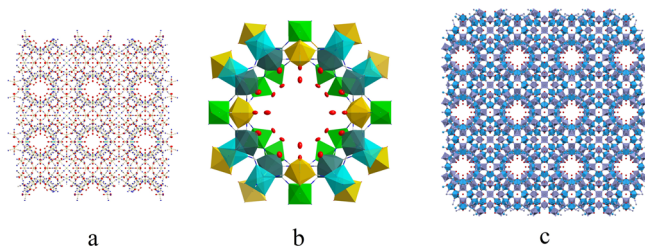

Figure 7. (a) The 3D network for **1** formed by linking two W and three Zn metal centers via cyano bridges, view along [001], (b) view along the channels present in the structure, with oxygen atoms O2, O3, O4, and O5 marked in the middle of channel, view along [001] (c) framework structure of **1** with metal centers highlighted with polyhedrons, view along [010]. The alternation of tungsten and zinc metallic centers is marked. Color codes for (b) yellow polyhedron − W1, dark blue polyhedron − W2, green polyhedron − Zn1, light blue polyhedron − Zn2, and red atom−oxygen, (c) gray polyhedron − W nodes, blue polyhedron − Zn nodes. All atoms are represented at 30% probability thermal ellipsoids.

the PLATON software,[54−57] and it is worth noting that expected volumes for solvent water molecules is 40 Å^3, and for small molecules (e.g., toluene) 100−300 Å^3. From the packaging analysis, it can be concluded that all water molecules, both coordinated to the Zn and W atoms and those freely filling the structure, are either directed to or fill the channels in the structure. In addition, it can be seen in the anion [W(CN)$_5$(OH)$_2$]$^{3-}$ that one of the OH ligands is directed to the inside of the channel. This means that in these channels there are as many as four different types of hydrogen atoms, which come from free H$_2$O (O2), from −OH (O3) coordinating W2 (2.110 Å), from H$_2$O (O4) coordinating Zn1 (2.245 Å), from H$_2$O (O5) coordinating W1 (2.255 Å), i.e., with very different distances from [metal centers, and thus with very different acidities. Thus, it can be assumed that structure of **1** is similar to that of zeolites, and probably the described salt could be used as a catalyst.[69,70]

Quantum Chemical Calculations. DFT geometry optimizations were performed on isolated anions [W(CN)$_5$(OH)$_2$]$^{3-}$ and [W(CN)$_5$(OH)(H$_2$O)]$^{2-}$ in order to

determine their preferred coordination geometries and thus rationalize the role played by the crystalline environment (see Supporting Information for detailed computational results).

The calculations predict both anions to have a singlet ground state, which is typical for W(IV) and Mo(IV) complexes with CN and O-based ligands. However, the calculations also demonstrate that lowest-energy structures of both anions are qualitatively different from the ideal pentagonal bipyramidal geometries present in the crystal structure part. The most stable computed geometry for isolated [W(CN)$_5$(OH)$_2$]$^{3-}$ and [W(CN)$_5$(OH)(H$_2$O)]$^{2-}$ anions, shown in Figure 8a,b, may
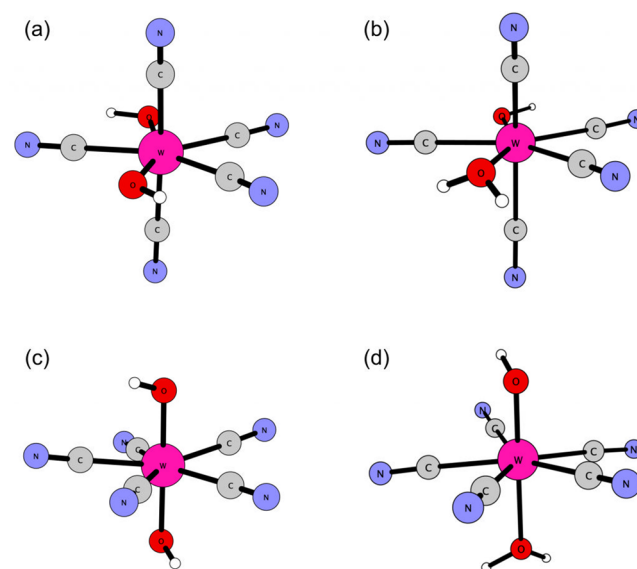
Figure 8. Optimized geometries of (a) [W(CN)$_5$(OH)$_2$]$^{3-}$ and (b) [W(CN)$_5$(OH)(H$_2$O)]$^{2-}$ ions in the most stable closed shell $S = 0$ state, and less stable conformations (c, d) of each ion (in the $S = 1$ state) corresponding to the pentagonal bipyramid geometry resembling that observed in the crystal structure.

be viewed as a highly distorted bipyramid, where two O atoms and three C atoms form the pentagonal base. This is arrangement of ligands is different from that in the crystal structure, where the pentagonal base is formed by five carbon atoms of the CN ligands, whereas oxygens are axial ligands (cf. Figure 2). The structures corresponding to the pentagonal bipyramid geometry as observed in the crystal structure, shown in Figure 8c,d, are predicted to be energetically less stable (see below and Table S2 for details). Thus, the presence of ideal pentagonal bipyramid geometries of [W(CN)$_5$(OH)$_2$]$^{3-}$ and [W(CN)$_5$(OH)(H$_2$O)]$^{2-}$ in the crystalline phase—which are not preferred for isolated anions—must be ascribed to the effect of intermolecular interactions, specifically the bridges formed by CN ligands to adjacent Zn^{2+} ions.

The computed energy differences between the most stable and the alternative structures are rather small (cf. Table S2). For [W(CN)$_5$(OH)$_2$]$^{3-}$, the lowest energy minimum consistent with the coordination geometry observed in the crystal structure is found at 11 kcal·mol^{-1} above the most stable structure. For [W(CN)$_5$(OH)(H$_2$O)]$^{2-}$, the corresponding energy difference is even smaller, 4 kcal·mol^{-1}. Moreover, all the identified energy minima are characterized by the presence of low-frequency vibrational modes (≤50 cm^{-1}, in some cases as small as a few cm^{-1}!), corresponding to ligand deformations which may interconvert different coordination polyhedra. The flatness of

potential energy surface (i.e., presence of multiple energy minima close in energy and low-frequency deformational modes) points to the picture of stereochemically labile complexes whose actual geometry (e.g., preferred in the crystal or solution) may be easily perturbed by intermolecular interactions.

Unfortunately, because of the large size of the unit cell and the presence of numerous heavy atoms, periodic DFT calculations (which may in principle rigorously account for these effects in the solid state) become prohibitively expensive. Although the presented molecular DFT calculations are not supposed to (and indeed do not) exactly reproduce the geometries of these anions found in the coordination polymer **1**, they are still able to reproduce the experimentally observed trends in the W–O bond lengths (cf. Table S2). For instance, the computed W–OH distance is shorter by ca. 0.08 Å in the $[W(CN)_5(OH)(H_2O)]^{2-}$ ion than in the $[W(CN)_5(OH)_2]^{3-}$ ion, whereas according to the crystal structure the difference is 0.076 Å (see above). The W–O bond lengths computed for pentagonal bipyramid structures are reasonably close (to within 0.01–0.07 Å) to the crystallographic ones, whereas those computed for the most stable distorted structures are noticeably shorter (by more than 0.1 Å). By contrast, the W–CN distances are reproduced less accurately, as might be expected given the involvement of CN ligands in bridging interactions with Zn^{2+}, which are not accounted for in the present calculations.

As mentioned in crystal structure description, the channels observed in **1** (Figure 8b) contain aqua ligands bound to different metal sites, W(IV) and Zn(II), which thus presumably have different acidities (related to deprotonation of coordinated H_2O to OH^- ligand). We computationally estimated the pK_a value of the $[W(CN)_5(OH)(H_2O)]^{2-}/[W(CN)_5(OH)_2]^{3-}$ acid–base pair using the proton exchange method[63] taking as reference the experimental pK_a value of 7.76 for $[W(CN)_4O(H_2O)]^{2-}/[W(CN)_4O(OH)]^{3-}$ acid–base pair.[71] Using the same reference, we also estimate the pK_a value of the Zn–OH_2 site present in the crystal structure of **1**. To this end, the $[Zn(NCH)_5(H_2O)]^{2+}/[Zn(NCH)_5(OH)]^+$ model was adopted in order to roughly describe the octahedral coordination environment of zinc. The estimated pK_a values are given in Table 2. Two values given for $[W(CN)_5(OH)(H_2O)]^{2-}/[W(CN)_5(OH)_2]^{3-}$ correspond, respectively, to open-shell singlet and triplet state, both with pentagonal bipyramid geometry (similar to that found in crystal structure). For closed-shell singlet distorted geometries, one would obtain

ΔpK_a of −6.67 and pK_a of 1.09; these values (not shown in Table 2) should not be treated as the measure of acidity of the $[W(CN)_5(OH)(H_2O)]^{2-}/[W(CN)_5(OH)_2]^{3-}$ system embedded in the crystal lattice of **1**.

The calculations thus point to conclusion that the H_2O ligand in pentagonal bipyramid $[W(CN)_5(OH)(H_2O)]^{2-}$ is slightly more acidic (by less than 0.5 pK_a unit) than that in the previously characterized pseudo-octahedral $[W(CN)_4O(H_2O)]^{2-}$ complex. Moreover, the H_2O ligand bound to the W(IV) site in $[W(CN)_5(OH)(H_2O)]^{2-}$ is predicted to be more acidic (by ca. one unit) than the H_2O ligand bound to the Zn(II) site. Such a result is qualitatively consistent with observation that both the Brønsted acid (W–H_2O) and its conjugated base (W–OH) forms in the crystal structure of **1**, whereas the Zn site is present only as the Brønsted acid Zn–H_2O form. The difference in acidic properties of aqua ligands in structure channels is similar to that found in zeolites and can be compared to that found in Si-MCM-48 zeolite, indicating that catalytic activity of **1** can be as rich as those found in the most popular industrial catalysts.[72]

CONCLUSIONS

We found that the very slow photolysis of the $[W(CN)_6(bpy)]^-/Zn^{2+}$ system results in formation of porous **1** with, for the first time detected seven coordinated pentacyanidotungstate(IV), enriching the discussion on the transition product of cyanidotungstate(IV, V) substitutional photolysis in aqueous media. A very rare cubic structure of $Pm\bar{3}n$ space group was created by the involvement of the cyanido ligands in a very complex 3D polymer with three different zinc coordination spheres and two tungstens. The water molecules are directed toward the created channels, and because of their different origins, significantly different acidic properties of the hydrogen suggest catalytic activity similar to zeolites. This will be part of future research. It was also found that the formation of cyanide bridges is responsible for the deformation of the most stable state of singlet W(IV) into triplet one and formation of the ideal pentagonal bipyramid geometry of the tungsten atom. Structure **1** is undoubtedly the first three-dimensional coordination polymer based on five node types (two W and three Zn) from the CN family of bridged coordination polymers. In addition, it is probably the first example that the ideal anion geometry is forced by a three-dimensional network of cyanide bridges. This fascinating compound requires further intensive research.

ASSOCIATED CONTENT

Ⓢ Supporting Information

The Supporting Information is available free of charge at https://pubs.acs.org/doi/10.1021/acs.cgd.0c00966.

> Selected crystal structure data (Table S1) as well as chemical calculation (Tables S2 and S3 and Figures S1 and S2) (PDF)

Accession Codes

CCDC 2002709 contains the supplementary crystallographic data for this paper. These data can be obtained free of charge via www.ccdc.cam.ac.uk/data_request/cif, or by emailing data_request@ccdc.cam.ac.uk, or by contacting The Cambridge Crystallographic Data Centre, 12 Union Road, Cambridge CB2 1EZ, UK; fax: +44 1223 336033.

Table 2. Computationally Estimated pK_a Values

acid–base pair (M-H_2O/M–OH)	$\Delta pK_a{}^a$	pK_a
$[W(CN)_4O(H_2O)]^{2-}$ $/ [W(CN)_4O(OH)]^{3-}$	/ --	7.76^b
$[W(CN)_5(OH)(H_2O)]^{2-}$ $/ [W(CN)_5(OH)_2]^{3-}$	-0.72^d	$7.04^{c,d}$
	-0.83^e	$6.93^{c,e}$
$[Zn(NCH)_5(H_2O)]^{2+}$ $/ [Zn(NCH)_5(OH)]^+$	/ 0.35	8.11^c

[a]Relative pK_a value of a given acid–base pair (i) with respect to the reference pair (ref) was calculated as $\Delta pK_a = \Delta \Delta E_a(i)/[RT \ln(10)]$ (T = 298 K) based on the energy difference $\Delta \Delta E_a(i) = \Delta E_a(i) - \Delta E_a(ref)$, where $\Delta E_a = E(M-OH) - E(M-H_2O)$. [b]Experimental value[70] used as the reference $pK_a(ref)$. [c]Computationally estimated using the calculated ΔpK_a value and the experimental reference, $pK_a = \Delta pK_a + pK_a(ref)$. [d]For S = 1 pentabpy structures. [e]For S = 0 pentabpy structures.

■ AUTHOR INFORMATION

Corresponding Author

Maciej Hodorowicz − *Faculty of Chemistry, Jagiellonian University, 30-387 Kraków, Poland;* ◉ orcid.org/0000-0003-4210-3625; Email: hodorowm@chemia.uj.edu.pl

Authors

Janusz Szklarzewicz − *Faculty of Chemistry, Jagiellonian University, 30-387 Kraków, Poland*

Mariusz Radoń − *Faculty of Chemistry, Jagiellonian University, 30-387 Kraków, Poland;* ◉ orcid.org/0000-0002-1901-8521

Anna Jurowska − *Faculty of Chemistry, Jagiellonian University, 30-387 Kraków, Poland*

Complete contact information is available at:
https://pubs.acs.org/10.1021/acs.cgd.0c00966

Notes

The authors declare no competing financial interest.

■ REFERENCES

(1) Szklarzewicz, J.; Samotus, A. Novel Cyano Complex of Tungsten (IV) with 2,2′-Bipyridyl. *Transit. Met. Chem.* **1988**, *13*, 69−71.

(2) Sieklucka, B.; Szklarzewicz, J.; Samotus, A. Photoreactivity of the (2,2′-bipyridyl) hexacyanotungstate (IV) ion in aqueous solution. *J. Photochem. Photobiol., A* **1993**, *70*, 35−38.

(3) Szklarzewicz, J. New cyano complex of W(V), AsPh$_4$[W(bpy)(CN)$_6$]; Reversible redox system W(bpy)(CN)$_6^-$ /W(bpy)(CN)$_6^{2-}$. *Inorg. Chim. Acta* **1993**, *205*, 85−89.

(4) Chilesotti, A. Di die sali complessi di molibdeno. *Gazz. Chim. Ital.* **1904**, *34*, 497−510.

(5) Rosenheim, A. Untersuchungen über die Halogenverbindungen des Molydäns und Wolframs. *Z. Anorg. Chem.* **1907**, *54*, 97−103.

(6) Rosenheim, A.; Garfunkel, A.; Kohn, F. Die Cyanide des Molybdäns. *Z. Anorg. Chem.* **1910**, *65*, 166−177.

(7) Collenberg, O. Über die Zersetzung der 4-wertigen Molybdän- und Wolfram-Octocyanide im Sonnenlicht. I. *Z. Anorg. Allg. Chem.* **1924**, *136*, 245−251.

(8) Bucknall, W. R.; Wardlaw, W. CCCXCVII. - The complex cyanides of molybdenum. *J. Chem. Soc.* **1927**, *0*, 2981−2992.

(9) Barbieri, G. A. Sulle reazioni cromatiche dei molibden-ott-cianuri. *Atti Accad. Lincei.* **1930**, *12*, 148.

(10) Adamson, A. W.; Welker, J. P.; Volpe, M. Exchange Studies with Complex Ions. I. The Exchange of Radiocyanide with Certain Heavy Metal Complex Cyanides1. *J. Am. Chem. Soc.* **1950**, *72*, 4030−4036.

(11) MacDiarmid, A. G.; Hall, N. F. Illumination—pH Effects in Solutions of Complex Cyanides1. *J. Am. Chem. Soc.* **1953**, *75*, 5204−5207.

(12) Adamson, A. W.; Sporer, A. H. Photochemistry of Complex Ions. I. Some Photochemical Reactions of Aqueous PtBr$_6^{-2}$, Mo(CN)$_8^{-4}$ and Various Co(III) and Cr(III) Complex Ions. *J. Am. Chem. Soc.* **1958**, *80*, 3865.

(13) Carassiti, V.; Claudi, M. Fotochimica di Sali complessi in soluzione. Nota I. Cinetica della decomposizione fotochimica e termica del molibdenottocianuro di potassio. *Ann. Chim. (Rome)* **1959**, *49*, 1697.

(14) Carassiti, V.; Balzani, V. Fotochimica di sali complessi in soluzione. Nota II. Rendimenti quantici e reazioni termiche di sostituzione nell'idrolisi acida di molibdenoottocianuro e di wolframoottacianuro di potassio. *Ann. Chim. (Rome)* **1960**, *50*, 630.

(15) Bertoluzza, A.; Carassiti, V.; Marinangeli, A. M. Fotochimica di sali complessi in soluzione.-Nota III. Studio quanto-simmetrico dei meccanismi di reazione dei processi fotochimici e termici nell'idrolisi del molibdenoottacianuro di potassio. *Ann. Chim. (Rome)* **1960**, *50*, 645−668.

(16) Carassiti, V.; Marinangeli, A. M.; Balzani, V. Fotochimica di sali complessi in soluzione.- Nota V. Cinetica dell'idrolisi basica fotochimica de molibdenottocianuro di potassio e wolframottacianuro di potassio. *Ann. Chim. (Rome)* **1960**, *50*, 790−805.

(17) Bertoluzza, A.; Carassiti, V.; Marinangeli, A. M. Contributi ad uno sviluppo modern del concetto di coordinazione, Nota X. L'ottocoordinazione nei complessi tetra e penta-OH-sostituiti del molibdenoottacianuro di potassio. *Ann. Chim. (Rome)* **1960**, *50*, 806−824.

(18) Moggi, L.; Bolletta, F.; Balzani, V.; Scandola, F. Photochemistry of co-ordination compounds—XV: Cyanide complexes. *J. Inorg. Nucl. Chem.* **1966**, *28*, 2589−2597.

(19) Balzani, V.; Manfrin, M. F.; Moggi, L. Definite evidence of a primary photoaquation reaction of the octacyanomolybdate (IV) complex anion. *Inorg. Chem.* **1969**, *8*, 47−49.

(20) Adamson, A. W.; Perumareddi, J. R. Photochemistry of Aqueous Octacyanomolybdate (IV) Ion, Mo(CN)$_8^{4-}$. *Inorg. Chem.* **1965**, *4*, 247−249.

(21) Perumareddi, J. R. Comment on the Supposedly Decacoordinate Intermediate in the Photolysis of Octacyano-Molybdate (IV) Complex Anion. *Z. Naturforsch., B: J. Chem. Sci.* **1966**, *21b*, 22−27.

(22) Jakób, W.; Jakób, Z. Investigations of the Photochemical Reacions of Octacyanomolybdates(IV) and Octacyanotungstates(IV) II. Octacyanomolybdate Complexes with NH$_3$, N$_2$H$_4$·H$_2$O. *Roczniki Chem.* **1962**, *36*, 601.

(23) Jakób, W.; Kosińska-Samotus, A.; Stasicka, Z.; Gołebiewski, A. On the Red Intermediate in a Photochemical Reaction of the Mo(CN)$_8^{4+}$ Ion. *Z. Naturforsch., B: J. Chem. Sci.* **1966**, *21*, 819−822.

(24) Mitra, R. P.; Sharma, B. K.; Mohan, H. Spectrophotometric, polarographic and titrimetric study of formation of a red intermediat in photolysis of octacyanomolybdic (4) acid. *Indian J. Chem.* **1969**, *7*, 1162.

(25) Mitra, R. P.; Sharma, B. K.; Mohan, H. Characterization and photolysis of octacyanomolybdic (IV) acid: isolation of a red photoproduct. *Can. J. Chem.* **1969**, *47*, 2317−2319.

(26) Wilson, R. D.; Sastri, V. S.; Langford, C. H. Sensitized Photolysis of Octacyanomolybdate (IV). *Can. J. Chem.* **1971**, *49*, 679−682.

(27) Mohan, H. Acid character of octacyanotungstic (IV) acid and isolation of a red product of its photodecomposition. *J. Inorg. Nucl. Chem.* **1976**, *38*, 1303−1305.

(28) Nya, A. E.; Mohan, H. Photochemistry of aqueous [W(CN)$_8$]$^{4+}$. *Polyhedron* **1984**, *3*, 743−747.

(29) Samotus, A.; Stasicka, Z.; Dudek, M.; Nadzieja, L. Investigations of the photochemical reactions of octacyanomolybdates(IV) and octacyanotungstates(IV). Part VI. Photolysis of [Mo(CN)$_8$]$^{4+}$ and [W(CN)$_8$]$^{4+}$ complexes in alkaline solution. *Roczniki Chem.* **1971**, *45*, 299−308.

(30) Samotus, A. Photochemical properties of octacyanotungstic acids. Part I. Photolysis of octacyanotungstic (IV) acid. *ibid* **1973**, *47*, 251−264.

(31) Stasicka, Z.; Bulska, H. Plash photolytic investigations of photochemistry of octacyanomolybdates. 1. Transient species in aqueous-slutions of [MoCN)$_8$]$^{4+}$. *Roczniki Chem.* **1973**, *47*, 1365−1374.

(32) Sieklucka, B.; Samotus, A. pH dependent photolysis of octacyanotungstate (IV) and kinetics of thermal reactions of photo-products. *J. Inorg. Nucl. Chem.* **1980**, *42*, 1003−1007.

(33) Dudek, M.; Samotus, A. Oxopentacyano-complexes of molybdenum (IV) and tungsten (IV) in photolysis of octacyanome-talates (IV). *Transition Met. Chem.* **1985**, *10*, 271−274.

(34) Matoga, D.; Szklarzewicz, J.; Samotus, A.; Burgess, J.; Fawcett, J.; Russell, D. R. Thermal and photochemical interaction of octacyano-metallates (IV),[M(CN)$_8$]$^{4+}$ (M = Mo or W) in the presence of pyrazine. *Transition Met. Chem.* **2001**, *26*, 404−411.

(35) Lippard, S. J.; Russ, B. J. Reactions of eight-coordinate metal cyanide complexes. I. Molybdenum (IV) and tungsten (IV) oxocyanide complexes. *Inorg. Chem.* **1967**, *6*, 1943−1947.

(36) Day, V. W.; Hoard, J. L. The structure of the trans-dioxotetracyanomolybdate (IV) ion in the crystalline salt NaK$_3$MoO$_2$(CN)$_4$·6H$_2$O. *J. Am. Chem. Soc.* **1968**, *90*, 3374−3379.

(37) Stadnicka, K. Crystal structure of Na$_3$MoO(OH)(CN)$_4$·4H$_2$O. *Roczniki Chem.* **1973**, *47*, 2021−2034.

(38) Robinson, P. R.; Schlemper, E. O.; Murmann, R. K. Characterization and structures of two protonated tetracyanomolybdenum (IV) oxy ions. *Inorg. Chem.* **1975**, *14*, 2035−2041.

(39) Arzoumanian, A.; Pierrot, M.; Ridouane, F.; Sanchez, J. Preparation and x-ray structure determination of penta-and tetracyano-oxomolybdenum (IV) anions. The influence of water on their reactivity. *Transition Met. Chem.* **1991**, *16*, 422−426.

(40) Wieghardt, K.; Backes-Dahmann, G.; Holzbach, W. Characterization of distortional isomers of the anions pentacyano-oxo-molybdate(IV) and of tetracyano-aqua-oxo-molybdate(IV) in the solid state. *Z. Anorg. Allg. Chem.* **1983**, *499*, 44−58.

(41) Szklarzewicz, J.; Matoga, D.; Samotus, A.; Burgess, J.; Fawcett, J.; Russell, D. R. Structure and Reactivity of (PPh$_4$)$_3$[W(CN)$_5$O]·7H$_2$O. Kinetics and Mechanism of the Reaction with Molecular Oxygen. *Croat. Chem. Acta* **2001**, *74*, 529−544.

(42) Stawski, T.; Szklarzewicz, J.; Lewiński, K. The transition products in substitutional photochemistry of [Mo(CN)$_8$]$^{4−}$ - theoretical approach. X-ray crystal structure of AsPh$_4$[W(bpy)(CN)$_6$]. *Transition Met. Chem.* **2006**, *31*, 353−361.

(43) Szklarzewicz, J.; Podgajny, R.; Lewiński, K.; Sieklucka, B. Basked wave-like 2-D coordination polymer generated by the self-assembly of [Mn(H$_2$O)$_6$]$^{2+}$ and geometrically anisotropic [W(CN)$_6$bpy]$^{2−}$ precursors. *CrystEngComm* **2002**, *4*, 199−201.

(44) Lim, K. S.; Hong, C. S. [W(CN)$_6$(L)]$^{1−}$/$^{2−}$ (L = bidentate ligand) as a useful building unit to construct molecule-based magnetic systems. *Dalton Trans.* **2013**, *42*, 14941−14950.

(45) Alexandru, M. G.; Visinescu, D.; Madalan, A. M.; Lloret, F.; Julve, M.; Andruh, M. [W(bipy)(CN)$_6$]$^−$: A Suitable Metalloligand in the Design of Heterotrimetallic Complexes. The First Cu^{II}Ln^{III}W^V Trinuclear Complexes. *Inorg. Chem.* **2012**, *51*, 4906−4908.

(46) Alexandru, M. G.; Visinescu, D.; Shova, S.; Lloret, F.; Julve, M.; Andruh, M. Two-Dimensional Coordination Polymers Constructed by [Ni^{II}Ln^{III}] Nodes and [W^{IV}(bpy)(CN)$_6$]$^{2−}$ Spacers: A Network of [Ni^{II}Dy^{III}] Single Molecule Magnets. *Inorg. Chem.* **2013**, *52*, 11627−11637.

(47) Radoń, M.; Rejmak, P.; Fitta, M.; Bałanda, M.; Szklarzewicz, J. How can [Mo^{IV}(CN)$_6$]$^{2-}$, an apparently octahedral (d)^2 complex, be diamagnetic? Insights from quantum chemical calculations and magnetic susceptibility measurements. *Phys. Chem. Chem. Phys.* **2015**, *17*, 14890−14902.

(48) Hodorowicz, M.; Szklarzewicz, J.; Jurowska, A. The versatility of lithium cation coordination modes in salts with [W(CN)$_6$(bpy)]$^{2−}$ anion. *CrystEngComm* **2020**, *22*, 3991.

(49) Szklarzewicz, J.; Fawcett, J.; Russell, D. R. Synthesis and X-ray crystal structures of Cs$_2$[W(bpy)(CN)$_6$]●2H$_2$O and (AsPh$_4$)$_2$[W-(bpy)(CN)$_6$]·3.5H$_2$O. *Transition Met. Chem.* **2004**, *29*, 56−60.

(50) Rigaku Oxford Diffraction. CrysAlis PRO. Rigaku OxfordDiffraction, Yarnton, England, 2015.

(51) Sheldrick, G. M. Crystal structure refinement with SHELXL. *Acta Crystallogr., Sect. C: Struct. Chem.* **2015**, *C71*, 3−8.

(52) Sheldrick, G. M. *SHELX2017, Programs for Crystal Structure Determination*; Universität Göttingen: Germany, 2017.

(53) Spek, A. L. PLATON SQUEEZE: a tool for the calculation of the disordered solvent contribution to the calculated structure factors. *Acta Crystallogr., Sect. C: Struct. Chem.* **2015**, *C71*, 9−18.

(54) Spek, A. L. Single-crystal structure validation with the program PLATON. *J. Appl. Crystallogr.* **2003**, *36*, 7−13.

(55) Spek, A. L. Structure validation in chemical crystallography. *Acta Crystallogr., Sect. D: Biol. Crystallogr.* **2009**, *D65*, 148−155.

(56) Spek, A. L. What makes a crystal structure report valid? *Inorg. Chim. Acta* **2018**, *470*, 232−237.

(57) Spek, A. L. checkCIF validation ALERTS: what they mean and how to respond. *Acta Crystallogr.* **2020**, *E76*, 1−11.

(58) Putz, H.; Brandenburg, K. *Diamond-Crystal and Molecular Structure Visualization*; Crystal Impact: Bonn, Germany, 2018.

(59) Adamo, C.; Barone, V. Toward reliable density functional methods without adjustable parameters: The PBE0 model. *J. Chem. Phys.* **1999**, *110*, 6158−6170.

(60) TURBOMOLE V7.4.1 (2019), a development of University of Karlsruhe and Forschungszentrum Karlsruhe GmbH, 1989−2007, TURBOMOLE GmbH, since 2007; available from http://www.turbomole.com (accessed 2020-05-21).

(61) Klamt, A.; Schuurmann, G. COSMO: a new approach to dielectric screening in solvents with explicit expressions for the screening energy and its gradient. *J. Chem. Soc., Perkin Trans. 2* **1993**, *2*, 799−805.

(62) Neese, F.; Schwabe, T.; Grimme, S. Analytic derivatives for perturbatively corrected 'double hybrid' density functionals: Theory, implementation, and applications. *J. Chem. Phys.* **2007**, *126*, 124115.

(63) Ho, J.; Coote, M. L. First-principles prediction of acidities in the gas and solution phase. *Wiley Interdiscip. Rev.: Comput. Mol. Sci.* **2011**, *1*, 649−660.

(64) Samotus, A.; Szklarzewicz, J.; Matoga, D. Coordination chemistry of Mo(IV) and W(IV) based on tetracyanodioxo precursors. *Bull. Polym. Acad. Sci. Chem.* **2002**, *50*, 145−164.

(65) Stadnicka, K. Crystal structure of Na$_3$MoO(OH)(CN)$_4$·4H$_2$O. *Roczniki Chem.* **1973**, *47*, 2021−2034.

(66) Dudek, M.; Kanas, A.; Samotus, A. Monomeric and dimeric products of protonation of dioxotetracyanometalates(IV)—II: Complexes of molybdenum(IV). *J. Inorg. Nucl. Chem.* **1979**, *41*, 1135−1142.

(67) Robinson, P. R.; Schlemper, E. O.; Murmann, R. K. Characterization and structures of two protonated tetracyanomolybdenum(IV) oxy ions. *Inorg. Chem.* **1975**, *14*, 2035−2041.

(68) Arzoumanian, A.; Pierrot, M.; Ridouane, F.; Sanchez, J. Preparation and x-ray structure determination of penta- and tetracyano-oxomolybdenum(IV) anions. The influence of water on their reactivity. *Transition Met. Chem.* **1991**, *16*, 422−426.

(69) Chester, A. W.; Derouane, E. G. *Zeolite Characterization and Catalysis*; Springer: New York, 2009; Vol. 360.

(70) Derouane, E. G.; Védrine, J. C.; Pinto, R. R.; Borges, P. M.; Costa, L.; Lemos, M.A.N.D.A.; Lemos, F.; Ribeiro, F. R. The Acidity of Zeolites: Concepts, Measurements and Relation to Catalysis: A Review on Experimental and Theoretical Methods for the Study of Zeolite Acidity. *Catal. Rev.: Sci. Eng.* **2013**, *55*, 454−515.

(71) Hejmo, E.; Kanas, A.; Samotus, A. Protonation constants of the trans-dioxotetracyanotungstate(IV) ion. *Bull. Acad. Polon. Sci., Ser. Sci. Chim.* **1973**, *21*, 311−317.

(72) Yu, K.; Kumar, N.; Aho, A.; Roine, J.; Heinmaa, I.; Murzin, D. Y.; Ivaska, A. Determination of acid sites in porous aluminosilicate solid catalysts for aqueous phase reactions using potentiometric titration method. *J. Catal.* **2016**, *335*, 117−124.